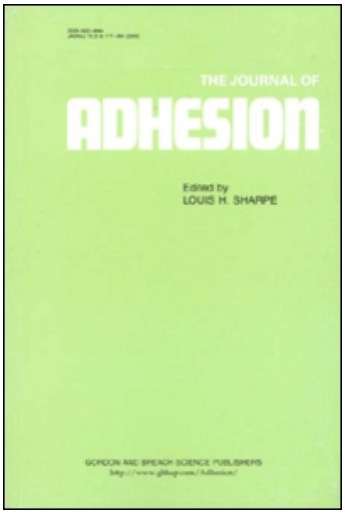


**The Journal of Adhesion**
Publication details, including instructions for authors and subscription information:
http://www.informaworld.com/smpp/title~content=t713453635

# Interfacial Chemistry of an Aluminum-to-EPDM Rubber Bonding System

Carol S. Hemminger[a]
[a] The Aerospace Corporation El Segundo, Carlifornia, USA

**To cite this Article** Hemminger, Carol S.(1994) 'Interfacial Chemistry of an Aluminum-to-EPDM Rubber Bonding System', The Journal of Adhesion, 47: 1, 51 — 64
**To link to this Article: DOI:** 10.1080/00218469408027089
**URL:** http://dx.doi.org/10.1080/00218469408027089

*J. Adhesion*, 1994, Vol. 47, pp. 51–64
Reprints available directly from the publisher
Photocopying permitted by license only

Printed in the United States of America

# Interfacial Chemistry of an Aluminum-to-EPDM Rubber Bonding System*

CAROL S. HEMMINGER**

*The Aerospace Corporation El Segundo, Carlifornia 90245, USA*

*(Received March 4, 1993; in final form August 27, 1993)*



During recent assessment of aging in aluminum-to-rubber bonds on stored solid rocket motors, corrosion and minor insulator debonds were observed. A test was conducted to study the progressive effect of exposure to high humidity on the bondline; elevated temperature was used to accelerate the aging. In a parallel test, samples were held at elevated temperature in a dry atmosphere. The test results were compared with the analyses of corroded and noncorroded hardware samples. The predominant corrosion product detected at the bondlines was aluminum oxide/hydroxide. In general, there was a very good correlation between the Cl:Al atomic percent ratio calculated from X-ray photoelectron spectroscopy analysis of the ruptured bondline surfaces and the visual characterization of the extent of corrosion. The Cl:Al ratio, which represented the ratio of primer to corrosion product at the locus of failure, varied from 0.4 to 47. The implications for metal-to-rubber bond fabrication and storage are discussed.

KEY WORDS Adhesion; corrosion; x-ray photoelectron spectroscopy (XPS); ethylene-propylene rubber; aluminum; bondline; surface analysis.

## INTRODUCTION

The metal casings of solid rocket motors (SRMs) are insulated with rubber. The rubber insulation is bonded to the metal with an adhesive system that includes a primer layer applied to the metal surface and one or more adhesive layers applied to the surface of the insulation. The resulting sandwich, metal/adhesive system/rubber, is cured at elevated temperature, in vacuum, to make the bond. During recent assessment of aging in aluminum-to-rubber bonds on stored SRMs, corrosion and minor insulator debonds were observed on three old motor cases. Unlike flight hardware, which is stored under controlled conditions, these motor cases had been stored in uncontrolled environments with high humidity exposures. It was thought possible that the atypical moisture exposure caused initiation and progression of the corrosion and debonds. Since failure

*Presented at the International Symposium on "The Interphase" at the Sixteenth Annual Meeting of The Adhesion Society, Inc., Williamsburg, Virginia, U.S.A., February 21–26, 1993.

**Mailing Address*: The Aerospace Corporation, Mail Stop M2/250, P.O. Box 92957, Los Angeles, CA 90009-2957, USA.

of an SRM metal-to-rubber bondline could result in catastrophic loss, further investigation has taken place.

When a similar corrosion problem was detected at SRM steel-to-rubber bondlines, a method for analysis was developed.[1] This method used rapid immersion of samples in liquid nitrogen to rupture the metal-to-rubber bondline. The temperature-stress rupture occurred predominantly near the metal/primer interface. The temperature-stress rupture technique takes advantage of the differences in the coefficients of thermal expansion of the materials at the bondline. The primer is relatively brittle compared with the adhesive and rubber layers, so it was not surprising that the rupture was observed at this layer. The liquid nitrogen used for rupture blanketed the ruptured surfaces from air exposure. This made it possible to transfer the samples to an inert atmosphere dry box with minimal surface oxidation from moisture or oxygen. Subsequent analysis of both sides of the ruptured steel-to-rubber bondlines was made by X-ray photoelectron spectroscopy (XPS). XPS surface composition and chemistry results for ruptured steel/rubber bondlines determined the locus of failure, and gave insight into the steel-to-primer adhesion and aging properties.

A modified temperature-stress rupture method has been developed for aluminum-to-rubber bondlines. Previous analyses of the bondlines had been made after standard peel or pull tests, which resulted in large areas of cohesive failure in the rubber, even where bondline corrosion was observed. The areas of cohesive failure obscured features of interest, and complicated analysis and data interpretation. The metal/primer interface of good adhesive bonds was virtually inaccessible for comparative study.

Aluminum bonded to rubber insulation is susceptible to moisture-induced corrosion. A test was conducted to study the progressive effect of exposure to high humidity on the bondline. This test was conducted at elevated temperature to accelerate aging. In a parallel test, other samples were held at elevated temperature in a dry atmosphere. The test results will be compared to the analyses of corroded and non-corroded hardware samples. The implications for metal-to-rubber bond fabrication and storage will be discussed.



## EXPERIMENTAL

The motor cases studied were approximately spherical, with aluminum annuli at the poles, known as "polar bosses," for mounting the igniter assembly and exhaust nozzle. Ethylene propylene diene monomer (EPDM) rubber was bonded to the aluminum (alloy 7175-T736) polar bosses with Chemlok 205® primer and Chemlok 234B® adhesive. Reference samples of all known starting materials were prepared for analysis. A fresh saw-cut surface from one of the polar bosses was used as a sample of aluminum alloy 7175-T736. It was sequentially cleaned ultrasonically in 1,1,1-trichloroethane and acetone, rinsed with acetone, and dried before analysis. A fresh-cut (acetone-cleaned Exacto blade) insulation surface from one of the polar boss samples was used as a reference material for EPDM rubber. Chemlok 205 primer and Chemlok 234B adhesive surfaces were prepared from fresh lots of material supplied by Lord Corporation (Erie, PA, USA). The primer was agitated in the can, then stirred thoroughly before being brushed onto stainless steel shim coupons. It was dark gray in color. Curing was

done in a vacuum oven for 65 min at 94°C, followed by 120 min at 154°C. This procedure was consistent with the specifications governing the bonding between the EPDM rubber insulation and the aluminum polar bosses. The Chemlok 234B adhesive surface was prepared and cured simultaneously, using the above technique. The adhesive was black in color. One sample surface each of primer and adhesive was gently scraped with an acetone-cleaned Exacto knife blade to provide roughened surfaces for comparison with the as-cured surfaces. Minor flaking of the Chemlok 205 and 234B was observed upon scraping.

Ten segments from five polar bosses were studied from three motor cases, as listed in Table I. The aluminum polar bosses had an annular shape. The inner and outer edges of the insulated boss surface were referred to as the ID edge and wingtip edge, respectively. The ID edge is exposed directly to the environment, and the wingtip edge is buried between the EPDM rubber and shear ply insulation layers. The segment dimensions varied because the polar bosses differ in size, as indicated in Table I by the boss diameter measured across the bolt circle. Samples were cut from polar boss segments to prepare coupons of appropriate size and shape for rupture and analysis. The first step was to cut a slice of the circumference approximately 13 mm wide. Such a polar boss slice is shown schematically in Figure 1. Insulation and aluminum were trimmed to about 3 mm thick, to give a sandwich about 6 mm thick. The sandwich was then cut lengthwise into four coupons, which ranged from about 13 mm × 13 mm × 6 mm to 13 mm × 25 mm × 6 mm in size, depending on the radius of the polar boss.

Six adjacent radial strips from the forward polar boss of motor case 2 (chosen for minimal bondline corrosion) were cut into a total of 24 coupons for the high-humidity test. Coupons were designated by column (strips 1 through 6) and row (A through D) notation, as seen schematically in Figure 2. The second and fifth radial strips were designated as the controls. The other 16 coupons were exposed to 100% relative humidity (RH) at 80° to 85°C. The coupons were placed on a stainless steel mesh on top of the ceramic tray in a glass desiccator. The bottom of the desiccator served as a reservoir for water. The sealed desiccator was placed in a temperature-controlled oven. Samples were removed after 1, 2, 4, 8, 14, 23, 32, 63, and 99 days by opening the oven, then the desiccator. The temperature in the furnace restabilized in about 30 min after

TABLE I
Segments of polar boss hardware studied

| SRM No. | Spec. No. | Polar Boss | Boss Diameter | Location on Polar Boss (Top Dead Center at 0°) |
|---|---|---|---|---|
| 1 | A5 | Forward | 14.6 in | Unknown |
| 1 | A6 | Forward | | ~90° from A5 |
| 1 | A1 | Aft | 28.8 in | ~330° |
| 1 | A2 | Aft | | ~210° |
| 1 | A12 | Aft | | Unknown |
| 2 | A7 | Forward | 11.4 in | ~180° |
| 2 | A8 | Forward | | Top Dead Center |
| 2 | A3 | Aft | 19.1 in | ~330° |
| 2 | A4 | Aft | | ~30° |
| 3 | A9 | Aft | 28.8 in | ~270° |

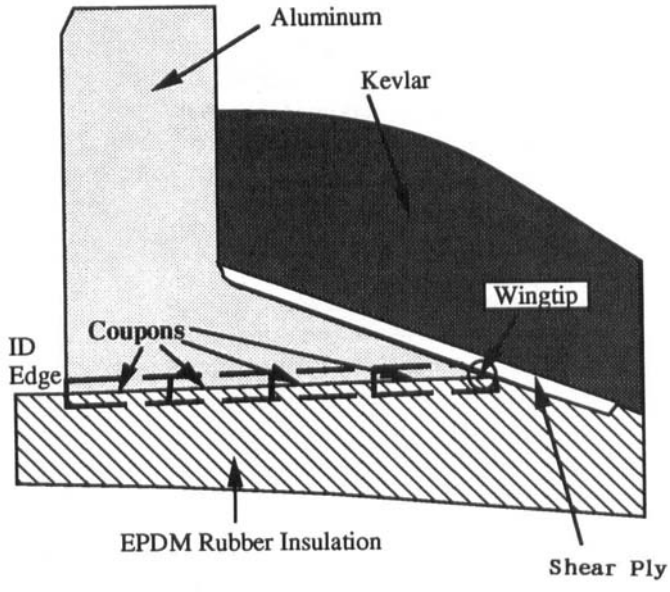


FIGURE 1 Schematic of polar boss slice, showing coupons for temperature-stress rupture.



sample removal. Moisture condensation was observed, but water did not collect heavily on the samples or stainless mesh.

A parallel, low-humidity test was conducted using a second sealed desiccator, with molecular sieve in the bottom, placed in the same oven at 80° to 85°C. Samples known to have pretest corrosion were cut from two aft polar boss segments. The effects of residual moisture in the rubber on bondline aging were thus investigated. Samples were removed from the dry desiccator for analysis after 49 and 99 days.

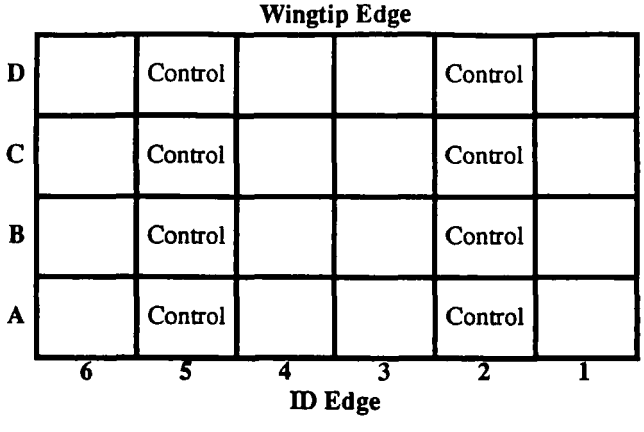


FIGURE 2 Schematic of forward polar boss test coupons from SRM case 2. Coupons were designated by column and row notation. The second and fifth radial strips were designated as the controls.

Rapid immersion of an entire aluminum/EPDM coupon into liquid nitrogen did not result in rupture. Rupture could be made predominantly near the Al/primer interface by holding the Al side of the sandwich in contact with liquid nitrogen. If rupture was not complete, the two halves were pulled apart, resulting in cohesive failure in the rubber in nonruptured areas. The nonruptured area was typically less than 10% of the total area and did not interfere with subsequent analysis. In cases where minimum exposure of the ruptured bondline to moisture and oxygen was desired, the entire sample was dropped into the liquid nitrogen as soon as rupture had occurred. Excess liquid nitrogen was decanted into a second Dewar. The Dewar with the immersed sample was then introduced into the antechamber of a dry box, where the remaining liquid nitrogen could be pumped away by the rough pump. Both surfaces exposed by the rupture were available for analysis by XPS to determine the locus of failure and the interfacial chemistry. The samples were subsequently mounted for analysis in the dry box and transferred to the XPS instrument under dry argon.

The samples were analyzed by XPS using a VG Scientific LTD ESCALAB MK II instrument. They were mounted on sample stubs with double-sided tape. Survey scans from 0 to 1100 eV binding energy were acquired with a Mg K$\alpha$ source to determine qualitatively the samples' surface composition. Analysis areas were about 4 mm × 5 mm in size, and analysis depth was about 50–100 Å. High-resolution elemental scans were subsequently run to obtain semiquantitative elemental analyses from peak area measurements and chemical state information from the details of binding energy and shape. Measured peak areas for all detected elements were corrected by elemental sensitivity factors (empirical, developed in this laboratory) before normalization to give surface atom %.



## RESULTS AND DISCUSSION

### 1 Reference Materials

The XPS surface composition data for the reference samples are shown in Table II. The nominal composition of 7175 aluminum alloy by weight is 90% Al, 5.6% Zn, 2.5% Mg,

TABLE II
XPS results: composition of reference materials

| | Surface Atom Percent, Normalized | | | | | | | | |
|---|---|---|---|---|---|---|---|---|---|
| Sample Description | Al | O | Si | Zn | Cl | S | C | N | Ti |
| 7175-T736 Aluminum Alloy | 28 | 45 | nd | 0.1 | 0.3 | 0.2 | 24 | 1.0 | nd |
| EPDM Insulation | nd | 2.8 | 1.6 | tr | 0.3 | 0.2 | 95 | 0.1 | nd |
| Chemlok: | | | | | | | | | |
| 205 Primer, As Cured | nd | 11 | 3.2 | 0.2 | 17 | tr | 68 | 0.8 | nd |
| 205 Primer, Scraped Surface | 0.4 | 11 | 0.9 | 0.3 | 18 | tr | 68 | 0.6 | 0.2 |
| 234B Adhesive, As Cured | nd | 2.9 | 0.9 | nd | 11 | nd | 85 | 0.2 | nd |
| 234B Adhesive, Scraped Surface | 0.2 | 8.4 | 1.9 | nd | 9.6 | 0.2 | 78 | 0.3 | nd |

tr = trace and nd = not detected

1.6% Cu, and 0.23% Cr. The fresh saw-cut surface analyzed by XPS had an aluminum oxide surface layer less than 100 Å thick: both zerovalent aluminum and aluminum oxide contributions were detected for the Al 2p high-resolution elemental peak. The fresh grit-blasted polar boss surfaces prepared for bonding should have had similar surface composition. The carbonaceous contamination was thin ( < 20 Å). A significant surface concentration of nitrogen (1 at.%) was detected. The Mg, Cu, and Cr components of the alloy were not detected by XPS on the reference surface.

The EPDM rubber insulation is primarily hydrocarbon in content, as reflected by the surface carbon concentration of 95 at.%. It has a silica hydrate filler, and low chlorine and sulfur concentrations. Both the primer and adhesive are characterized by relatively high concentrations of chlorinated hydrocarbon. XPS did not detect chloride ion (peak binding energy 198–199 eV) mixed with the chlorine bonded to carbon (peak binding energy 200–201 eV), but its presence below the detection limit is possible. The primer contains zinc and titanium oxides ( the latter detected by XPS only on the scraped surface) among its suspended solids, while the adhesive does not contain these oxides. The nitrogen concentration was higher in the primer than in the adhesive. The as-cured surfaces and the scraped surfaces (representing "bulk" material) were similar for both the primer and adhesive.



## 2 Polar Boss Samples

Visual inspection of the ruptured polar boss sample bondlines showed that rupture appeared to occur, predominantly, close to the Al/primer interface. Significant flecks of primer/adhesive did remain on the Al surface. On ruptured "good" bonds, there was no visual sign of Al surface corrosion, even after the ruptured bondline was exposed to atmosphere for several weeks. The EPDM side of the rupture appeared uniformly dark gray in color. Ruptured "poor" bonds had a spotted appearance on both the Al and EPDM sides of the interface, and a high density of corrosion product was observed on both surfaces under an optical microscope. Some ruptured bondlines were considered "fair" in appearance. The fair bondlines had a lightly mottled Al surface, but the rubber surface appeared relatively clean. Small patches of corrosion product were observed on both surfaces under an optical microscope. Figure 3 shows the progression from fair to poor in the condition of a bondline from the aft polar boss of motor case 1 (segment Al2), moving from the ID edge (left side) to the midsection. The progression is most readily seen in the exposed EPDM rubber surfaces of the coupons.

The appearance of the ruptured bondlines was distinctly different from the pulled-rubber bondlines, both for "good" and "poor" bonds. In the case of a pulled good bond, the rupture appeared to be cohesive within the EPDM. In the case of a pulled poor bond, rupture took place near the Al surface. The surface of both Al and insulation appeared spotted, as with a corrosion product, but a large area percentage of the Al side was covered with the Chemlok system after the insulation was pulled. Shallow surface lapping and polishing of the covered Al surface areas showed a high density of corrosion product infiltrated into the primer layer but not extending into the adhesive layer.[2]

The XPS surface composition data for an illustrative subset of the polar boss samples are shown in Table III. Information is provided in Table III about the *approximate*

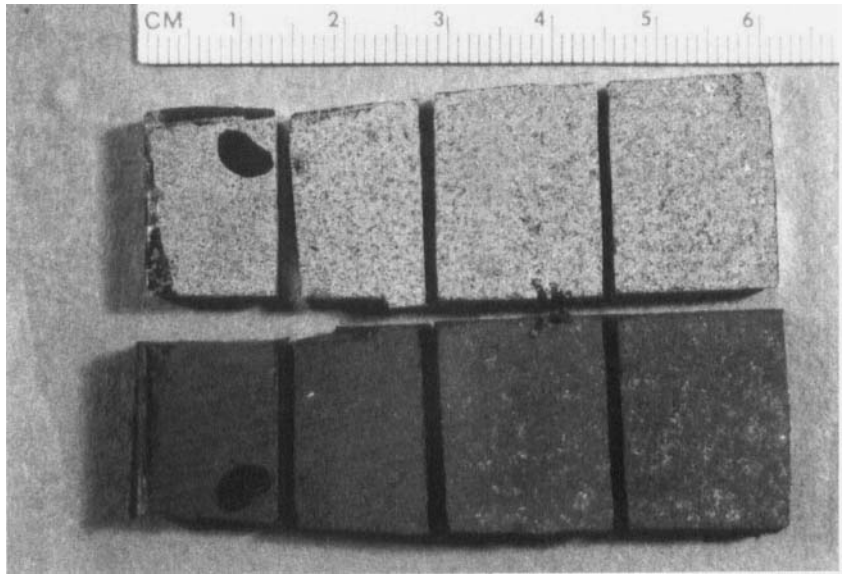


FIGURE 3 Progression from fair to poor in the condition of a bondline from the aft polar boss of motor case 1 (segment A12), moving from the ID edge (left side) to the midsection. The progression is most readily seen in the exposed EPDM rubber surfaces of the coupons.



radial analysis position referenced to the ID edge of the polar boss as "0%" (the ID and wingtip analysis areas are at "5%" and "95%", respectively, in this scheme). All of the data were consistent with the observation that temperature-stress rupture occurs, predominantly, close to the aluminum-to-primer interface. From 1 to 13 at.% Al was detected on each ruptured surface. The zinc concentrations, typically 0.5 to 1.5 at.%, and high chlorine concentrations, 5 to 24 at.%, were indicative of the primer component. The aluminum and EPDM sides of the ruptured interface had similar composition, with a 20% to 40% decrease in the relative Al concentration on the EPDM surface being the most consistent difference (note that only one of the EPDM surfaces analyzed is included in Table III). After this observation was made, further analysis of the EPDM rubber was limited in order to minimize sample outgassing contamination of the vacuum chamber used for XPS analysis. It was also observed that the composition of ruptured aluminum-to-insulation bondlines did not appear to change significantly upon exposure to air, even after several weeks.

Significant differences in surface composition were observed between noncorroded and corroded polar boss bondline surfaces. The variation in surface concentrations of Al, O, Cl, and C were all notable. The Cl:Al atomic concentration ratio is listed in Table III, along with a simplified description of the visual appearance of the bondline as predominantly "good," "fair," or "poor," with respect to observed extent of corrosion. In general, there was an excellent correlation between the calculated Cl:Al at.% ratio, and the visual characterization of the extent of corrosion. The Cl:Al ratio, which represents the primer-to-aluminum compound ratio at the locus of failure, varied from 0.4 to 47. With only a few exceptions, surfaces with a fair to good, noncorroded

TABLE III
XPS results for polar boss samples: elemental composition data

| SRM No. | Spec. No. | Polar Boss | Side | Analysis Position* | Surface Atomic Percent, Normalized Al | O | Si | Zn | Cl | S | C | N | Cl:Al | Bond Line |
|---|---|---|---|---|---|---|---|---|---|---|---|---|---|---|
| 1 | A5 | Fwd | Al | ID | 6.0 | 20 | 0.7 | 1.0 | 14 | 0.4 | 57 | 0.4 | 2.4 | Fair |
| 1 | A5 | Fwd | Al | mid(20%) | 5.8 | 20 | 0.6 | 1.1 | 14 | 0.6 | 56 | 1.4 | 2.5 | Fair |
| 1 | A5 | Fwd | Al | mid(30%) | 7.2 | 22 | 0.7 | 1.3 | 15 | 0.6 | 53 | 1.0 | 2.0 | Fair |
| 1 | A5 | Fwd | Al | mid(45%) | 5.8 | 18 | 0.7 | 1.0 | 15 | 0.6 | 58 | 1.3 | 2.6 | Fair |
| 1 | A5 | Fwd | Al | mid(80%) | 6.4 | 21 | 0.7 | 1.0 | 15 | 0.4 | 55 | 0.8 | 2.3 | Fair |
| 1 | A5 | Fwd | Al | wingtip | 6.2 | 19 | 0.5 | 0.7 | 16 | 0.3 | 56 | 0.9 | 2.6 | Fair |
| 1 | A1 | Aft | Al | ID | 6.7 | 25 | 0.6 | 1.0 | 6.1 | 0.7 | 59 | 1.4 | 0.9 | Fair |
| 1 | A1 | Aft | Al | ID | 7.0 | 26 | 0.5 | 1.3 | 7.7 | 0.5 | 56 | 1.0 | 1.1 | Poor |
| 1 | A1 | Aft | Al | mid(20%) | 6.3 | 26 | 0.4 | 1.3 | 5.5 | 0.8 | 59 | 1.3 | 0.9 | Poor |
| 1 | A1 | Aft | Al | mid(40%) | 9.1 | 29 | 0.1 | 1.1 | 5.8 | 1.0 | 52 | 1.3 | 0.6 | Poor |
| 1 | A1 | Aft | EPDM | mid(40%) | 6.8 | 24 | 1.0 | 0.9 | 5.5 | 1.2 | 59 | 2.1 | 0.8 | Poor |
| 1 | A1 | Aft | Al | mid(80%) | 9.8 | 28 | 0.6 | 1.2 | 5.0 | 1.4 | 52 | 1.7 | 0.5 | Poor |
| 1 | A1 | Aft | Al | wingtip | 7.8 | 25 | 0.4 | 1.1 | 7.7 | 1.0 | 55 | 2.0 | 1.0 | Fair |
| 1 | A12 | Aft | Al | ID | 4.8 | 19 | 0.7 | 0.9 | 12 | 0.7 | 61 | 1.2 | 2.6 | Fair |
| 1 | A12 | Aft | Al | mid(25%) | 7.0 | 27 | 0.3 | 1.3 | 9.4 | 0.7 | 54 | 1.2 | 1.3 | Fair |
| 1 | A12 | Aft | Al | mid(40%) | 9.4 | 30 | 0.6 | 1.2 | 5.7 | 1.0 | 50 | 1.4 | 0.6 | Poor |
| 1 | A12 | Aft | Al | mid(60%) | 11 | 33 | 0.2 | 1.2 | 3.8 | 1.2 | 48 | 1.2 | 0.4 | Poor |
| 2 | A8 | Fwd | Al | ID | 2.0 | 12 | 3.4 | 0.7 | 19 | 0.4 | 62 | tr | 9.6 | Good |
| 2 | A8 | Fwd | Al | mid(20%) | 2.3 | 11 | 0.9 | 0.8 | 20 | 0.4 | 64 | 0.6 | 8.6 | Good |
| 2 | A8 | Fwd | Al | mid(30%) | 3.3 | 11 | 0.7 | 0.9 | 11 | 0.4 | 72 | 0.5 | 3.4 | Good |
| 2 | A8 | Fwd | Al | mid(45%) | 3.1 | 11 | 0.6 | 1.0 | 20 | 0.6 | 63 | 0.9 | 6.5 | Good |
| 2 | A8 | Fwd | Al | mid(80%) | 3.9 | 12 | 0.5 | 0.6 | 19 | 0.4 | 62 | 0.4 | 5.0 | Good |
| 2 | A8 | Fwd | Al | wingtip | 2.0 | 8.6 | 0.6 | 0.8 | 18 | 0.5 | 69 | 0.5 | 8.9 | Good |
| 2 | A4 | Aft | Al | ID | 3.3 | 18 | 3.2 | 0.6 | 11 | 0.3 | 63 | 0.9 | 3.4 | Fair |
| 2 | A4 | Aft | Al | mid(20%) | 6.9 | 24 | 1.1 | 0.6 | 8.2 | 0.3 | 58 | 0.9 | 1.2 | Fair |
| 2 | A4 | Aft | Al | mid(40%) | 9.3 | 28 | 0.3 | 0.6 | 8.5 | 0.6 | 52 | 1.4 | 0.9 | Poor |
| 2 | A4 | Aft | Al | mid(80%) | 8.5 | 27 | 0.3 | 0.7 | 7.3 | 0.7 | 54 | 1.5 | 0.9 | Poor |
| 2 | A4 | Aft | Al | wingtip | 3.4 | 16 | 0.4 | 0.8 | 16 | 0.5 | 63 | 0.9 | 4.6 | Fair |
| 3 | A9 | Aft | Al | ID | 0.5 | 5.8 | 0.3 | 0.2 | 24 | 0.4 | 68 | 0.9 | 47 | Good |
| 3 | A9 | Aft | Al | mid(20%) | 3.4 | 11 | 0.3 | 0.6 | 19 | 0.7 | 63 | 1.4 | 5.6 | Fair |
| 3 | A9 | Aft | Al | mid(30%) | 3.9 | 12 | 0.4 | 0.6 | 20 | 1.0 | 61 | 1.0 | 5.2 | Fair |
| 3 | A9 | Aft | Al | mid(45%) | 4.2 | 13 | nd | 0.6 | 21 | 1.0 | 60 | 0.8 | 4.9 | Fair |
| 3 | A9 | Aft | Al | mid(55%) | 5.4 | 18 | 0.5 | 0.6 | 14 | 1.6 | 58 | 1.9 | 2.5 | Fair |
| 3 | A9 | Aft | Al | mid(70%) | 3.3 | 14 | 0.7 | 0.7 | 18 | 0.9 | 61 | 1.4 | 5.3 | Fair |

* Analysis Position is defined as an approximate percentage of the distance from the ID edge (5%) to the wingtip (95%) along a polar boss raidus.
tr = trace and nd = not detected.

appearance had Cl:Al ratios greater than 2, and surfaces with a poor, corroded appearance had Cl:Al ratios less than 1. The change in this ratio was related to changes in both the Al and Cl concentrations. As the bondline changed from good to poor, the Al oxide/hydroxide concentration increased significantly, and the primer concentration, represented by the covalently-bonded Cl signal, decreased.

The observation of higher concentrations of aluminum oxide/hydroxide at the rupture zone suggested that the temperature-stress rupture progressed most readily through areas of thickened aluminum oxide/hydroxide if it was present. It is reasonable to expect that areas of thickened, brittle aluminum oxide/hydroxide would be more susceptible to temperature-stress rupture than the primer layer or a noncorroded aluminum-to-primer bond. When corrosion product was not present, the high Cl:Al ratios of the rupture surfaces implied that fracture was primarily cohesive in the primer. The areas of corrosion product were also noted to be correlated with pockets of primer pullout from the rubber side of the rupture.[3] This would be consistent with the infiltration of corrosion product into a network of cracks in the primer layer, as seen in Figure 4, which was observed in cross-section studies of the corroded bondlines.[2] It is possible that crack defects in the primer layer determine the initiation sites for the metal corrosion.

All samples from the forward polar bosses, and from the aft polar boss of motor case 3, had a relatively noncorroded appearance and low to moderate concentrations of corrosion product. The aft polar boss segments analyzed from motor cases 1 and 2 were



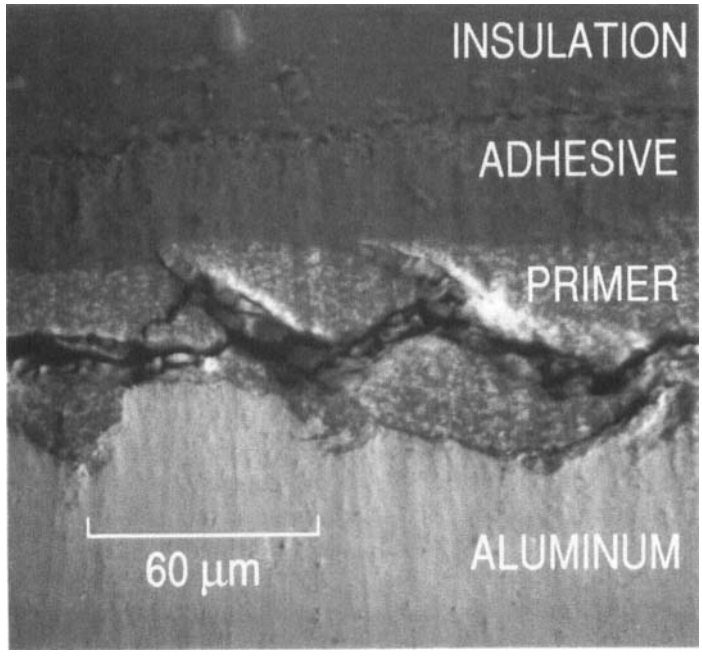


FIGURE 4 SEM micrograph showing primer layer cracks filled with corrosion in a cross-section study of a corroded bondline.

characterized by the appearance of corrosion over the entire midsection of the ruptured aluminum-to-insulation bondline. The ID edges and wingtip edges of the aft segments appeared less corroded than the midsections. In all analyses, the aluminum was detected only as oxide and/or hydroxide, and chloride ion was below detection. Minimal corrosion at the ID edges, which are exposed to environmental moisture, strongly suggests a manufacturing-process-related initiation of corrosion. This is supported by the significant differences observed between the forward and aft bosses exposed to the same storage environments. This, in turn, implies that properly-stored flight motors, regardless of age, need to be inspected for the presence of corrosion.

A few additional comments can be made about the XPS results. On average, the N and S concentrations tended to be somewhat higher on the corroded surfaces than on the noncorroded surfaces. Some "sulfate" (S 2p binding energy at about 269 eV) was observed on most of the samples analyzed, typically about 25% of the total sulfur. The concentration of zinc oxide was higher on most of the ruptured surfaces than on the reference primer samples. This might be due to the details of how temperature-shock rupture occurs through the primer (*e.g.*, rupture might occur preferentially near the zinc oxide particles), or there may be some segregation of zinc oxide at the interface.



## 3 Test Samples

The control coupons from strips 2 and 5 were analyzed to determine the baseline interfacial composition and chemistry, and to examine the condition of the bondline in the chosen segment. Strip 5 was relatively corrosion-free. Strip 2 had corrosion product at some areas of the locus of failure. The 1-day exposure sample, coupon 3B, revealed a similar corrosion pattern on part of the coupon, indicating some pre-existing corrosion on strip 3. Strip 1 was also suspected to have corrosion. Subsequent test coupons, after the 1-day exposure, were selected from strips 4 and 6, through the 63-day exposure.

Heavy contamination of the ID edge of coupon 2A was seen by optical microscopy and XPS analysis. The contaminant was primarily a silicone. Fluorocarbon was also detected, and metal debris was seen on the magnified surface. Some silicone contamination was also detected by XPS on the ID edge of control coupon 5A, leading to speculation that a contamination smear had occurred along the ID edge from at least strips 2 to 5.

The XPS composition data for the Al surfaces of the control coupons are shown in Table IV. The Cl:Al ratios for the strip 5 control surfaces were all greater than 5, indicating that little corrosion product is present at the bondline. The Cl:Al ratios for the strip-2 surfaces indicate minimal corrosion at the wingtip edge but an increase in aluminum oxide/hydroxide at part of the midradius towards the ID edge. Although corrosion product was seen with an optical microscope, it was relatively light. Cl:Al ratios less than 1 were not measured. At the ID edge of coupon 2A the silicone and fluorocarbon contamination obscured the aluminum and chlorine signals, so that a Cl:Al ratio was not obtained.

Samples were removed from exposure to 100% RH at 80° to 85°C after 1, 2, 4, 8, 14, 23, 32, 63, and 99 days. After 1 day of exposure, the outer surfaces of the aluminum coupons were dull and slightly darkened compared with the controls. After 4 days of exposure, significant corrosion product was observed over the entire outer aluminum surface area. After 8 days of exposure, large blisters of corrosion product had developed,

TABLE IV
XPS results for control test coupons: elemental composition data for aluminum side of thermal-stress-ruptured metal/insulation bondline

| Sample Description | | Surface Atom Percent, Normalized | | | | | | | | |
|---|---|---|---|---|---|---|---|---|---|---|
| Coupon | Analysis Position* | Al | O | Si | Zn | Cl | S | C | N | Cl:Al |
| 5A | ID | 3.0 | 15 | 4.3 | 0.8 | 18 | 0.3 | 59 | nd | 5.9 |
| | 20 | 3.0 | 14 | 0.6 | 0.9 | 17 | 0.5 | 64 | 0.4 | 5.5 |
| 5B | 30 | 2.6 | 13 | 0.6 | 0.7 | 20 | 0.3 | 62 | tr | 8.0 |
| | 45 | 3.1 | 12 | 0.6 | 0.8 | 18 | 0.3 | 64 | 0.7 | 5.9 |
| 5C | 55 | 2.4 | 12 | 0.7 | 0.8 | 18 | 0.3 | 65 | tr | 7.5 |
| | 70 | 2.4 | 12 | 0.9 | 0.7 | 20 | 0.3 | 63 | tr | 8.4 |
| 5D | 80 | 2.5 | 13 | 0.7 | 0.7 | 20 | 0.3 | 63 | 0.6 | 8.1 |
| | Wingtip | 1.8 | 9.8 | .07 | 0.7 | 23 | 0.3 | 64 | tr | 13 |
| 2A | ID | nd | 23 | 23 | nd | nd | nd | 51 | 0.3 | ** – |
| | 20 | 5.3 | 17 | 0.8 | 0.8 | 16 | 0.4 | 59 | 0.8 | 3.0 |
| 2B | 30 | 7.1 | 21 | 0.4 | 0.7 | 13 | 0.4 | 56 | 1.3 | 1.8 |
| | 45 | 5.3 | 17 | 0.5 | 0.8 | 14 | 0.3 | 62 | 0.6 | 2.6 |
| 2C | 55 | 4.0 | 17 | 1.3 | 1.0 | 16 | 0.1 | 60 | 0.9 | 3.9 |
| | 70 | 3.0 | 16 | 0.4 | 0.8 | 18 | 0.4 | 61 | 0.4 | 6.0 |
| 2D | 80 | 3.7 | 14 | 0.5 | 0.8 | 19 | 0.2 | 61 | 0.5 | 5.1 |
| | Wingtip | 2.0 | 11 | 0.5 | 0.8 | 23 | 0.3 | 62 | 0.4 | 11 |

tr = trace (< 0.5%) and nd = not detected
* Given as a percentage distance from the ID edge to the wingtip.
The ID and wingtip locations are 5% and 95%, respectively.
** 2.1% F also detected at this heavily-contaminated analysis area.



and pitting was observed. The pitting and corrosion continued to worsen on the outer surfaces of the coupon, but no debonds were observed until samples were removed after a 63-day exposure. At that time, coupons 3A and 4A were observed to have a debond along the ID edge. The debonded area corresponded to the area where a contamination smear had apparently occurred along the ID edge from at least strips 2 to 5. No debonds were observed when the 99-day-exposure samples were removed from the desiccator.

Evidence of corrosion over a small percentage of the total surface area at the ruptured bondline was first found after the 8-day and 14-day exposures. The initial corrosion spots were small, less than a few tenths of a millimeter in diameter, and were all within a few millimeters of the coupon edges. This pattern suggested diffusion of moisture along the bondline from the edge rather than from the backside of the insulation. Corrosion spots this close to the ID edge were not typical on hardware samples. No corrosion product was observed along the very edge of the ruptured surfaces, indicating that corrosion did not progress as a uniform "front" as moisture diffused from the exposed cut bondline edge. The surface composition of the 8-day exposed ruptured surface gave no indication of corrosion development. Decreases in the Cl:Al ratio were measured for edge areas with corrosion spots on the 14-day exposed sample.

Corrosion was found at the centers of the coupons exposed for 23 days and longer. Although the corrosion areas had increased in size, some to a millimeter in diameter, they were still discrete spots that did not generally coalesce. Even after the longest exposure time, resistant, noncorroded areas of many square millimeters were observed. The Cl:Al ratio in these areas was greater than 3.

XPS analyses are shown in Table V for six different areas on the ruptured aluminum surface of the sample pulled after 32 days of exposure. The first four areas were about 4 × 5 mm in size; areas 5 and 6 were about 1.5 mm in diameter, centered on corrosion spots. The Cl:Al ratios revealed the heterogeneity of this surface. Area 1 had minimal corrosion, comparable with noncorroded bondlines described above. Area 4 contained numerous corrosion spots and had a composition comparable with corroded hardware. Corrosion spots 5 and 6 had the highest concentrations of Al and O and the lowest concentration of Cl from the primer.

The concentrations of both sulfur and zinc increased significantly, by factors of 2 and 1.5, respectively, compared with the controls, on the average-area compositions of the samples exposed 8 days or longer. The increase in sulfur and zinc concentrations was even more pronounced in some of the small-area analyses of the corrosion product: by factors of 4 and 2, respectively. Analysis of the S 2p binding energy showed that the predominant chemical state of sulfur changed from "organic" (bonded predominantly to carbon and hydrogen, S 2p binding energy about 163 eV) to "sulfate" (highly oxidized, S 2p binding energy about 169 eV). The sulfur oxidation was presumably due to exposure to water at the bondline. The increase in sulfur and zinc concentrations at the ruptured surfaces could be promoted by the elevated temperature of the test exposures and/or by the effects of moisture diffusion. It is not known if the sulfate is acting as a corrosive agent on the aluminum. The surface compositions imply that the corrosion product is predominantly aluminum oxide/hydroxide.

Microscopic examination showed that pockets of primer pullout were associated with the corrosion spots. Corrosion product had expanded into cracks through the primer layer towards the adhesive and rubber layers. Upon rupture, the primer layer in areas of heavy corrosion remained on the aluminum side, as seen in Figure 5; intact primer was observed on the insulation side in noncorroded areas. This suggested that corrosion may initiate at pre-existing defect sites correlated with small brittle cracks in the primer layer. Areas that were corrosion resistant, after the longest exposure times and near ID and wingtip edges of the hardware, may have a relatively defect-free primer layer that prevents moisture from reaching the aluminum surface. Cross section analyses of intact bondlines[2] did not detect any cracks through the primer layer that were not filled with corrosion product. The failure of corrosion spots to coalesce readily

TABLE V
XPS results: aluminum surface, 32 days of exposure

| | Surface Atom Percent, Normalized | | | | | | | | |
|---|---|---|---|---|---|---|---|---|---|
| Area | Al | O | Si | Zn | Cl | S | C | N | Cl:Al |
| 1 | 2.2 | 11 | 1.5 | 0.8 | 20 | 0.6 | 64 | tr | 9.2 |
| 2 | 5.2 | 17 | 1.3 | 1.3 | 16 | 0.4 | 58 | 0.7 | 3.0 |
| 3 | 7.4 | 26 | 1.6 | 1.5 | 12 | 0.7 | 49 | 0.9 | 1.7 |
| 4 | 12 | 31 | 1.2 | 1.4 | 9.2 | 0.5 | 44 | 0.5 | 0.8 |
| 5 | 20 | 38 | nd | 1.3 | 6.8 | 1.2 | 33 | nd | 0.3 |
| 6 | 21 | 47 | 0.9 | 1.5 | 4.8 | nd | 25 | nd | 0.2 |

tr = trace and nd = not detected

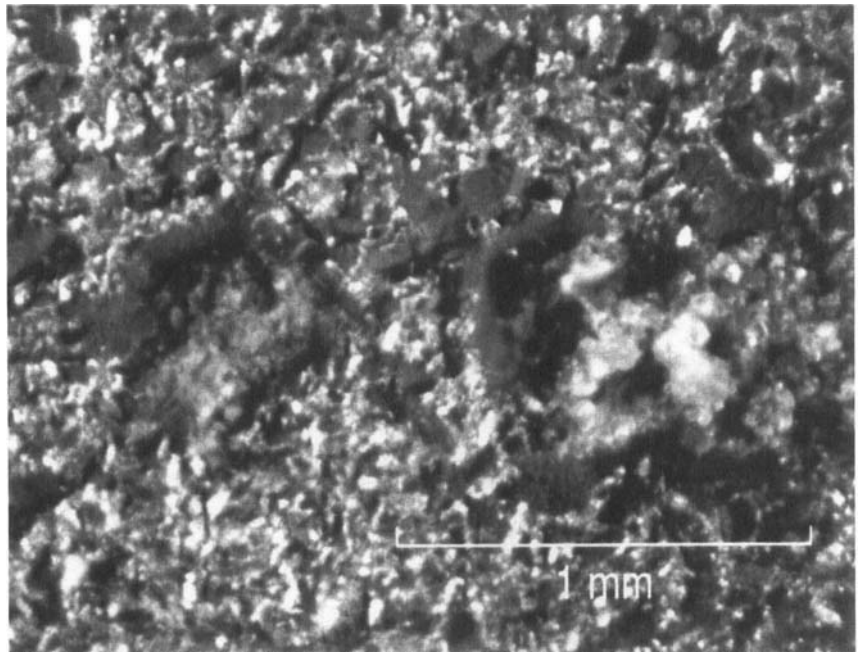


FIGURE 5 Optical micrograph of primer pockets remaining in areas of heavy corrosion on the aluminum side of the interface after bondline rupture. Sample exposed for 23 days.



suggests that large-area debonds in hardware are unlikely to result from moisture-induced corrosion at the Al/rubber bondline.

Samples known to have pre-existing bondline corrosion were ruptured after 49 and 99 days at 80° to 85°C in a dry atmosphere. They showed no change in appearance compared with previously-analyzed hardware, and significant changes in the XPS characterization details were not noted. This suggests that residual moisture in the rubber does not pose a serious threat to hardware stored under dry conditions. In particular, hardware which has been inspected and found to have "acceptable" levels of bondline corrosion is unlikely to deteriorate catastrophically if stored properly.

## SUMMARY

A temperature-stress rupture method using partial immersion in liquid nitrogen was developed for aluminum bonded to rubber. Subsequent XPS analysis of ruptured bondlines showed that the locus of failure for noncorroded samples was predominantly near the Al/primer interface. The primer was identified by its high concentration of chlorinated hydrocarbon. The corroded bondline sections had significantly higher concentrations of aluminum oxide/hydroxide than the noncorroded areas and lower concentrations of primer material detected by XPS. In general, there was a very good correlation between the calculated Cl:Al at.% ratio and the visual characterization of

the extent of corrosion. Surfaces with a noncorroded appearance had Cl:Al ratios greater than 2, and surfaces with a corroded appearance had Cl:Al ratios less than 1. The predominant corrosion product detected was aluminum oxide/hydroxide. XPS did not detect chloride ion mixed with the chlorine bonded to carbon from the primer on any of the polar boss samples, but its presence at low concentration was not ruled out.

A test was conducted to study the progressive effect of water on the aluminum/rubber bondline. Evidence of corrosion over a small percentage of the total surface area at the ruptured bondline was found after 8-day and 14-day exposures to 100% RH at 80° to 85°C. The observed corrosion pattern near the coupon edges suggested diffusion of moisture along the bondline from the edge rather than from the backside of the rubber insulation. General lack of corrosion along the very edge indicated that corrosion did not progress as a uniform "front" as moisture diffused from the exposed cut bondline edge. Corrosion was found at the centers of the coupons exposed for 23 days and longer, but the corrosion areas were still discrete spots that did not generally coalesce. Even after the longest exposure time, resistant, noncorroded areas were observed. Increases in sulfur and zinc concentrations were measured with the appearance of corrosion product, and the predominant chemical state of sulfur changed from organic to sulfate. It is not known if the sulfate acted as a corrosive agent on the aluminum. Microscopic examination showed that pockets of primer pullout were associated with the corrosion spots. Corrosion product had expanded through the primer layer towards the adhesive and rubber layers. Upon rupture, the primer layer in areas of heavy corrosion remained on the aluminum side; intact primer was observed on the insulation side in noncorroded areas. This suggests that corrosion may initiate at pre-existing defect sites correlated with small brittle cracks in the primer layer. Cracks filled with corrosion product were observed in metallographic cross sections through the bondline on corroded hardware.



## Acknowledgements

This work was supported by Air Force Space and Missile Systems Center, contract F04701-88-C-0089. The author gratefully acknowledges J. M. Marcus for preparation of the test coupons and N. Marquez for the optical microscopy.

## References

1. S. Zacharius, W. Stuckey, G. Cagle, and C. Hemminger, presented at The 13th Annual Meeting of the Adhesion Society, Savannah, GA, February 1990.
2. S. W. Frost, T. D. Le, and R. A. Brose, The Aerospace Corporation Report No. TOR-92(2464)-2, 15 June 1992.
3. C. S. Hemminger and N. Marquez, The Aerospace Corporation Report No. TOR-92(2464)-4, 30 September 1992.